RSC Applied Polymers

ROYAL SOCIETY OF CHEMISTRY

PAPER

View Article Online
View Journal | View Issue

Cite this: *RSC Appl. Polym.*, 2023, **1**, 304

Porous bioelectronic substrates for simple electrochemical conjugation and subsequent, controlled electrochemical release of antisense oligonucleotide drug†

Sara Beikzadeh,[a,b,d] Devon T. Bryant,[a] Alireza Akbarinejad,[c] Lisa I. Pilkington,[a] Anthony R. J. Phillips[d] and Jadranka Travas-Sejdic *[a,b]

Materials and methods that enable selective and controllable conjugation and release of chemical and biological substances are in demand for various applications, such as drug delivery, cell stimulation, and cancer therapy. Stimuli-responsive systems for controlled release and enhanced drug efficacy are of particular interest. We have here developed an electrochemically addressable system for the specific conjugation and release of connexin43 antisense as a wound-healing agent. The system is based on a conducting terpolymer, P(EDOT-*co*-EDOTSAc-*co*-EDOTEG), which was coated onto both carbon cloth and highly porous electrospun substrates. We optimized the conducting terpolymer composition and characterized and compared the terpolymer-coated substrates. The conductive terpolymer contains EDOTSAc, which has an acetylthiomethyl group that can be transformed into a "free" thiol. This thiol can undergo reversible oxidation/reduction cycles at moderate potentials (+1.0 and −0.8 V, respectively) to enable electrochemical conjugation and controlled release. The system was able to quickly conjugate (1 min) and release (5 min) a model thiol molecule in a highly controllable manner, which was demonstrated with, and compared between, carbon cloth and electrospun fiber substrates. Furthermore, successful conjugation and release of connexin43 antisense were demonstrated. Overall, this electrochemical system offers a porous and flexible platform with electrochemically stimulated conjugation and release capabilities that holds significant potential for wound dressing applications.

Received 16th May 2023,
Accepted 28th August 2023

DOI: 10.1039/d3lp00047h

rsc.li/rscapplpolym

Introduction

There is a significant demand for materials and methods that allow for the selective and controllable capture and release of chemical and biological substances.[1–3] Research efforts have been directed toward the capture and release of a wide range of clinically relevant targets, such as proteins,[4,5] small drug molecules,[6,7] extracellular vesicles (EVs),[8,9] cells[1,10–12] and DNA[5,13] for a number of applications, including drug delivery,[14] cell stimulation[15] and cancer therapy.[16,17] Stimuli-responsive systems for gene and drug delivery have gained widespread interest as they offer controlled and sustained release, enhanced drug efficacy and reduced potential side effects.[1,5,18,19] Different methods have been developed to capture and release oligonucleotides by using stimuli, such as heat,[20] light,[5,21,22] aminosilane-modified bacterial magnetic particles,[23] modified Fe_3O_4/Au nanoparticles,[24] host–guest binding and electrostatic interaction[5,25] and surfactants.[26]

The electrochemically-induced release is a promising method for delivering chemical and biological entities rapidly and easily, using electrical potential or current to control cargo release without additives.[1,8,27] This approach requires electrically conductive materials that undergo oxidative/reductive cycles at mild potentials to efficiently capture and release the desired cargo.[28,29] For instance, Gao *et al.*[30] developed an electrochemical system for controllable capture and release of cancer cells using β-cyclodextrin (β-CD) and ferrocene (Fc) through a host–guest interaction. Cancer cells were modified with a polyethylenimine (PEI) polymer scaffold conjugated with Fc and co-linked with folic acid (FA). Reduction potential facilitated binding of uncharged Fc to immobilized β-CD on

[a]*School of Chemical Sciences, The University of Auckland, 23 Symonds Street, Auckland, 1023, New Zealand. E-mail: j.travas-sejdic@auckland.ac.nz*
[b]*MacDiarmid Institute for Advanced Materials and Nanotechnology, Kelburn Parade, Wellington, 6140, New Zealand*
[c]*Faculty of Engineering, Chemical and Materials Engineering, 5 Grafton Rd, Auckland 1010, New Zealand*
[d]*School of Biological Sciences, The University of Auckland, 3A Symonds Street, Auckland 1010, New Zealand*

† Electronic supplementary information (ESI) available. See DOI: https://doi.org/10.1039/d3lp00047h

the electrode surface, while oxidation potential dissociated the Fc-β-CD complex, thereby releasing the captured cells.

Abidian *et al.*[29] demonstrated a noteworthy approach to achieve controlled release from electrospun nanofibers composed of biodegradable poly(L-lactide) infused with dexamethasone. Their study involved the electrochemical deposition of a PEDOT conducting-polymer layer around the drug-loaded nanofibers. By applying an external electrical stimulation of +1 V to the PEDOT nanotubes, they effectively controlled the release of dexamethasone from the nanofibers.

Yuan *et al.*[31] synthesized non-covalently grafted polymers that are capable of self-assembling into micellar structures using β-cyclodextrin modified dextran (Dex-CD) and Fc terminated poly(ε-caprolactone) (PCL-Fc). The presence of an Fc group on the polymer allowed for potential-controlled modulation of hydrophilicity/hydrophobicity, enabling self-assembly and disassembly of the micelles. These micellar structures were explored as drug carriers for controlled-release applications.[31] Jiao *et al.*[32] integrated poly(*N*-isopropylacrylamide) hydrogel with a redox-responsive cross-linkers (*N*,*N*′-bis(acryloyl)cystamine, BAC) into a microfluidic device using photopolymerization. The hydrogel "dots" captured and released modified protein bovine serum albumin (BSA) by reforming redox-responsive disulfide bonds, thereby altering the hydrogen dot densities. While several methodologies have been developed recently for electrochemical release and delivery, they have limitations, such as the need for high release potentials and the complexity of fabrication.[1]

On-skin electronics have attracted significant attention and have been successfully utilized in a wide range of applications in human healthcare, human–machine interfaces, soft robotics, biological studies and augmented reality.[33–35] Despite significant recent developments, current on-skin devices are not sophisticated enough to measure complex physiological conditions. Chronic non-healing wounds exemplify a challenge for existing skin electronics, as they fail to provide an efficient solution.[36] This can be attributed to the intricate and dynamic nature of the wound-healing process, which is influenced by various factors. These factors encompass patient co-morbidities like diabetes and renal failure, as well as local wound characteristics such as growth factors, inflammatory mediators, and the presence of microbial burden.[37–39] Modulation of the wound environment by delivery of therapeutics in a controlled and personalised manner offers a different approach to treating chronic wounds.[40–42] Electrochemical techniques offer new opportunities for the retention of wound healing agents and bioactives and their controlled release to the wound surface.[27,43]

We have recently reported the development of a sensor for detecting biothiols based on a conductive polymer called poly (EDOT-thioacetate-*co*-EDOT).[28] This sensor utilizes the thioacetate moieties on the conducting polymer, which can be electrochemically deprotected to the corresponding thiols that can then form disulfide bonds upon electrochemical oxidation, allowing for the reversible capture and release of biothiols.[28] We have further developed this technology by using similar conductive polymer-coated substrates, to create an electrochemically switchable interface for the controlled capture and release of biological targets, such as human cancer cells, antibodies and extracellular vesicles (EVs) from breast cancer cells and placenta.[1,8,9,44,45]

Building on these previous works, we present a system with the conducting-polymer deposited onto carbon cloth (CC) and electrospun polycaprolactone (PCL) fibers (EF) mats. The benefit of CC and electrospun fibers are that they have high surface porosity, conductivity and biocompatibility[8,9] which render them suitable surface-conforming materials for wound healing applications, where these properties are key attributes. Through optimization of the terpolymer composition and its redox chemistry, the terpolymer [P(EDOT-*co*-EDOTSAc-*co*-EDOTEG)] was electropolymerized on the CC and EF mats substrates. These were investigated as novel platforms to actively electrochemically control the delivery of wound healing agents using simple redox chemistry.

Anti-sense oligodeoxynucleotides (ODNs) are synthetic DNA molecules that allow for *in situ*, site-specific downregulation of connexin protein expression.[46] The downregulation of connexin expression in wound healing has multiple therapeutic potentials, including wound healing, reduced inflammation, decreased scar formation, and skin rejuvenation and thickening.[46] Our platform enables the controlled and customized direct delivery of connexin43 antisense for various wound conditions, especially chronic wounds where connexin43 expression is dysregulated.[47,48] Matching the release rate of the connexin43 antisense molecule to the specific healing stages and conditions of the patient's wounds has the potential to enhance the effectiveness of personalized wound treatments.

Here, we successfully demonstrate that the conductive terpolymer-coated substrates enable electrochemical conjugation and on-demand release of connexin43 oligodeoxynucleotides *via* reversible oxidation/reduction cycles at +1.0 V and −0.8 V (*vs.* Ag/AgCl), respectively. These findings open a door to future studies towards the delivery of connexin43 and other therapeutics to wounds, including chronic wounds.

Experimental section

Materials

Epichlorohydrin, triethylene glycol monomethyl ether, potassium *tert*-butoxide (^{t}BuOK), polycaprolactone (PCL, MW 80 000), 2-mercaptoethanol, (2ME), 6-mercaptohexanoic acid (MHA), *n*-hydroxysuccinimide (NHS), DL-alanine, fetal bovine serum (FBS), glutaraldehyde, paraformaldehyde (PFA), lithium perchlorate, sodium chloride, and calcein-AM were purchased from Sigma-Aldrich. Thioacetic acid s-potassium salt, dimethoxythiophene, 3,4-ethylenedioxythiophene, *p*-toluenesulfonyl chloride, 1-ethyl-3-(3-dimethylaminopropyl)-carbodiimide (EDC) were purchased from AK Scientific. *o*-Phthalaldehyde was purchased from Acros Organics. Thiolated-ODN of connexin43 antisense (Nexagon) (5′-GTAATTGCGGCAAGAAGAATTGTTTCTGTC-3′) was supplied

from Alpha DNA. All buffer tablets were supplied by Sigma-Aldrich.

Synthesis of ((2,3-dihydrothieno[3,4-*b*][1,4]dioxin-2-yl)methyl) ethanethioate, EDOTSAc

EDOTSAc was synthesized in three steps from epichlorohydrin according to the previously reported method in our group.[28] First, the epoxide in epichlorohydrin underwent a ring-opening to provide the corresponding diol, which was then reacted with dimethoxythiophene, forming EDOT-CH_2-Cl. To install the thiol functionality, EDOT-CH_2-Cl was reacted with potassium thioacetate, forming EDOTSAc.

Synthesis of 2-(2,5,8,11-tetraoxadodecyl)-2,3-dihydrothieno[3,4-*b*][1,4]dioxine, EDOTEG

EDOTEG was synthesized in two steps according to a previously reported method in our group.[28] First, ethylene glycol was reacted with tosyl chloride to form the corresponding tosylate, which was then reacted with hydroxymethyl-EDOT in the presence of ^{t}BuOK to provide EDOTEG.

Fabrication of the electrospun PCL fibre mat

12% of PCL was added to a mixture of dimethylformamide : tetrahydrofuran (1 : 1 vol : vol) and stirred at room temperature until completely dissolved. PCL solution was drawn into a 5 mL glass syringe with a 21G metallic needle and placed in the syringe pump component of an electrospinning setup (Adelab Scientific). The electrospinning was carried out at 15 kV, a flow rate of 2 mL h^{-1} and a distance of 15 cm. The fibers were homogeneously collected on a paper-covered rotating drum at a speed of 200 rpm. 8 mL of PCL solution was electrospun in total (total time of 4 hours). The PCL electrospun fiber (EF) mat membrane was then sputter-coated on both sides with a 20 nm gold layer at a speed of 4 nm min^{-1} using a Q150R sputter coater (Quorum).

Preparation of carbon cloth

Carbon cloth ELAT – Hydrophilic Plain Cloth (Woven Carbon Fiber) was purchased from the Fuel Cell Store. Carbon cloth substrate (10 × 5 mm) was cut and immersed in ethanol for 30 min and sonicated for 5 min to remove any impurities. Following this, the CC was then immersed in deionised water for 30 min, sonicated for 5 min and air-dried on a tissue.

Electrodeposition of P(EDOT-*co*-EDOTSAc-*co*-EDOTEG) terpolymer

All solutions used for electrochemistry were degassed with nitrogen for 15 minutes prior to the experiments. A three-electrode electrochemical setup was used to deposit P(EDOT-*co*-EDOTSAc-*co*-EDOTEG) onto a 5 × 5 mm area of the prepared carbon cloth and the gold-coated electrospun substrate using CHI660 Instruments electrochemical workstation, where these substrates were used as the working electrode, a platinum mesh as the counter electrode and Ag/AgCl (3 M NaCl-BASi) as the reference electrode. The polymerization was performed at a potential of 1.5 V (*vs.* Ag/AgCl,+0.230 V *vs.* SHE) for 1 min in 0.1 M $LiClO_4$ water : acetonitrile (1 : 1 vol : vol) solution containing different concentrations of EDOTSAc, EDOT and EDOTEG. The P(EDOT-*co*-EDOTSAc-*co*-EDOTEG)-coated substrate was then washed with water : acetonitrile (1 : 1 vol : vol) solution three times to remove the electrolyte and any unreacted monomers.

Conjugation of thiolated-ODsN with and without fluorescence tag (5′-end thiol and 3′ end fluorescein) and their release

The terpolymer P(EDOT-*co*-EDOTSAc-*co*-EDOTEG) underwent reduction to form P(EDOT-*co*-EDOTSH-*co*-EDOTEG) when a potential of −0.8 V (*vs.* Ag/AgCl) was applied onto the working electrode for 30 s in phosphate-buffered saline (PBS) solution. The reduced terpolymer, P(EDOT-*co*-EDOTSH-*co*-EDOTEG), then underwent oxidation when a potential of +1.0 V (*vs.* Ag/AgCl) was applied for 60 s in the solution of thiolated connexin43 antisense (Nexagon) (50 μg mL^{-1}, 2 mL) to form a disulfide bond between the thiolated-ODN and the thiol moiety on EDOTSH mer. The substrates were then washed thoroughly with deionized water (5 mL) and PBS solution (5 mL) to remove the non-specifically attached ODN. The next day, the substrates were immersed in 2 mL of PBS for 10 min to let the unbound ODN wash off the substrate. The conjugated ODNs were then released into a PBS buffer by applying a potential of −0.8 V (*vs.* Ag/AgCl) for 300 seconds. The fluorescence signal from the release solution was measured using the PerkinElmer spectrofluorometer (model LS 55B) at an excitation wavelength of 493 nm, with a scan rate of 200 nm min^{-1} and excitation and emission bandpasses of 10 nm. The concentration of released non-flurescent ODN was measured by Implen NanoPhotometer N60/NP80 (NanoDrop), which measures the absorption of light at 260 nm to determine the amount of ODN in a sample. The detection range of the instrument for ODN was 1 ng μl^{-1} to 16 500 ng μl^{-1} and 2 μl of the release solution has been used to measure the concentration of the released ODN.

FTIR spectroscopy

FTIR spectra of terpolymer P(EDOT-*co*-EDOTSAc-*co*-EDOTEG) electrodeposited carbon cloth substrate were recorded using a PerkinElmer FTIR spectrometer within a range of 4000–400 cm^{-1}.

Scanning electron microscopy (SEM)

SEM images were obtained using on a JCM-6000 Versatile Benchtop SEM from JEOL. Only the unmodified PCL electrospun fibers were coated gold-coated with a 20 nm gold layer at a speed of 4 nm min^{-1} using a Q150R sputter coater (Quorum) prior to SEM imaging.

Conductivity measurements

The conductivity of samples was measured using a four-point probe conductivity meter (Janel RM2), taking an average of 5 points per electrode.

Statistical analysis

The unpaired *t*-test, one-way ANOVA (α = 0.05) and Tukey's HSD multicomparison tests were used to test for statistical significance between the groups. Results are reported as an average ± standard deviation (SD). The graphs are reported with error bars representing the SD. All statistical analyses were performed using GraphPad Prism 8.

Results and discussion

Design, fabrication and characterization of conjugation/release system using terpolymer-coated conductive substrates

Two distinct conducting substrates were fabricated to construct materials capable of electrochemically-controlled conjugation and release. Fig. 1 shows the steps involved in each of the substrate's fabrication processes. Gold-coated electrospun PCL fiber mat (EF) and carbon cloth (CC) were used as the starting substrates. PCL is a nontoxic and biocompatible polymer that could be easily electrospun into a porous fiber mat membrane.[1,49] The EF was made electrically conductive by sputter-coating both sides of the mat with a 20 nm-thick layer of gold. CC electrodes were washed to remove any impurities before the electropolymerization step. Electropolymerization of three monomers: 3,4-ethylenedioxythiophene (EDOT), an acetylthiomethyl-substituted EDOT *S*-[(2,3-dihydrothieno[3,4-*b*][1,4]dioxin-2-yl)methyl] ethanethioate, denoted as "EDOTSAc", and EDOT substituted with three ethylene glycol units 2-(2,5,8,11-tetraoxadodecyl)-2,3-dihydrothieno[3,4-*b*][1,4]dioxine, denoted as "EDOTEG", was performed onto 0.5 ×

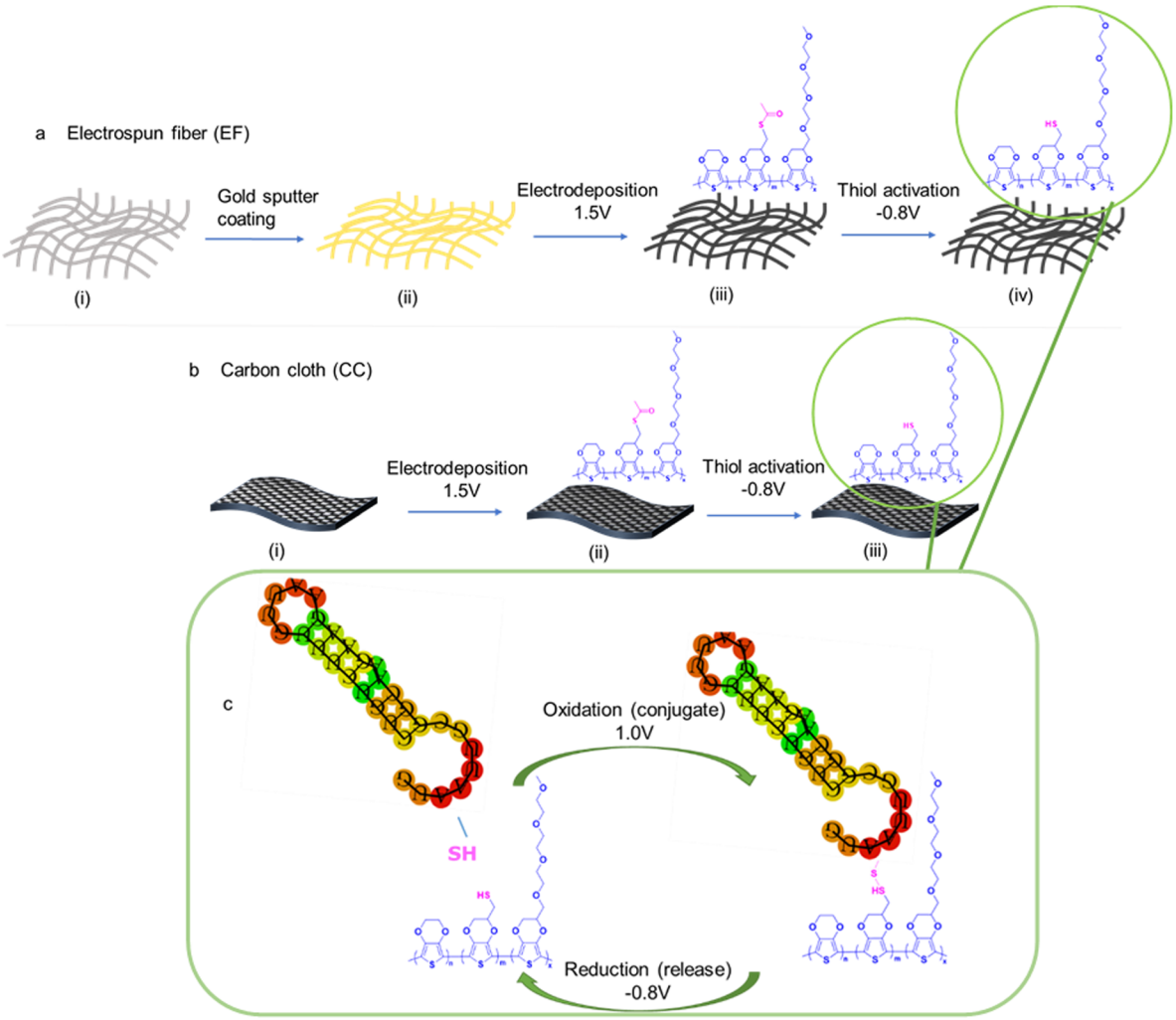

Fig. 1 Schematics showing: (a) The fabrication procedure of the electrospun fiber (EF) mat coated with the terpolymer: (i) PCL membrane electrospinning, (ii) sputter coating of gold on PCL membrane, (iii) P(EDOT-*co*-EDOTSAc-*co*-EDOTEG) terpolymer electropolymerization, (iv) thiol activation by electrochemical reduction of P(EDOTSAc) to P(EDOTSH). (b) The fabrication procedure of the carbon cloth substrate with electropolymerized P(EDOT-*co*-EDOTSAc-*co*-EDOTEG) terpolymer (ii), and after thiol activation by electrochemical reduction of P(EDOTSAc) to P(EDOTSH) (iii). (c) Electrochemical coupling of thiol-functionalised connexin43 through the oxidative formation of disulphide and cleavage by reduction of the disulfide, on both the P(EDOTSH) EF and P(EDOTSH) CC substrates. (The figure is a schematic representation and may not be drawn to an exact scale.)

0.5 cm pieces of gold-coated EF and 0.5 × 0.5 cm pieces of CC using chronoamperometry. The incorporation of the EDOTSAc mer enables the conjugation and subsequent release functionality of these substrates through electrochemically forming and breaking disulfide bonds. The EDOTEG was used to increase the substrate's hydrophilicity and antifouling properties, and the unmodified EDOT was used as a spacer for the other two functionalized EDOTs.[28]

The electropolymerization of the terpolymer P(EDOT-*co*-EDOTSAc-*co*-EDOTEG) on CC and PCL EF mats was conducted in 0.1 M $LiClO_4$ water : acetonitrile (1 : 1 vol : vol) containing 5.3 mM EDOTSAc (5%), 40 mM EDOT (80%) and 8 mM EDOTEG (15%). The potentiodynamic polymerizations of the terpolymers were performed in a potential range from −0.2 V to +1.25 V (*vs.* Ag/AgCl) at a 100 mV s^{-1} scan rate (Fig. 2a) or using a constant potential at +1.5 V for 2 min (Fig. 2b). The electropolymerization voltammograms of the terpolymer onto CC showed increased currents on the subsequent potential sweep cycles, suggesting the successful coating of the terpolymer onto the CC (Fig. 2a). The onset potential of electropolymerization for the terpolymer was +1.1 V.

It was shown earlier by us that a potential of −0.8 V (*vs.* Ag/AgCl) reduces the acetylthiomethyl moiety on the EDOTSAc to a thiol (denoted as EDOTSH);[28] here −0.8 V was applied for an optimized time of 30 s for the activation of the thiol (Fig. 2c). Thiolated-ODN were then conjugated to the P(EDOT-*co*-EDOTSH-*co*-EDOTEG) through the electro-oxidative formation of a disulfide covalent bond between the two thiol groups by applying a potential of +1.0 V for 60 s (Fig. 2d). The conjugated ODN was shown to be able to be released by applying a potential of −0.8 V (*vs.* Ag/AgCl) for 300 s (Fig. 2e).

Water contact angle measurements showed a significant decrease in contact angle from 112.45 ± 2° for CC and 68.22 ± 4° for gold-coated EF to 0.0° upon the electrodeposition of the

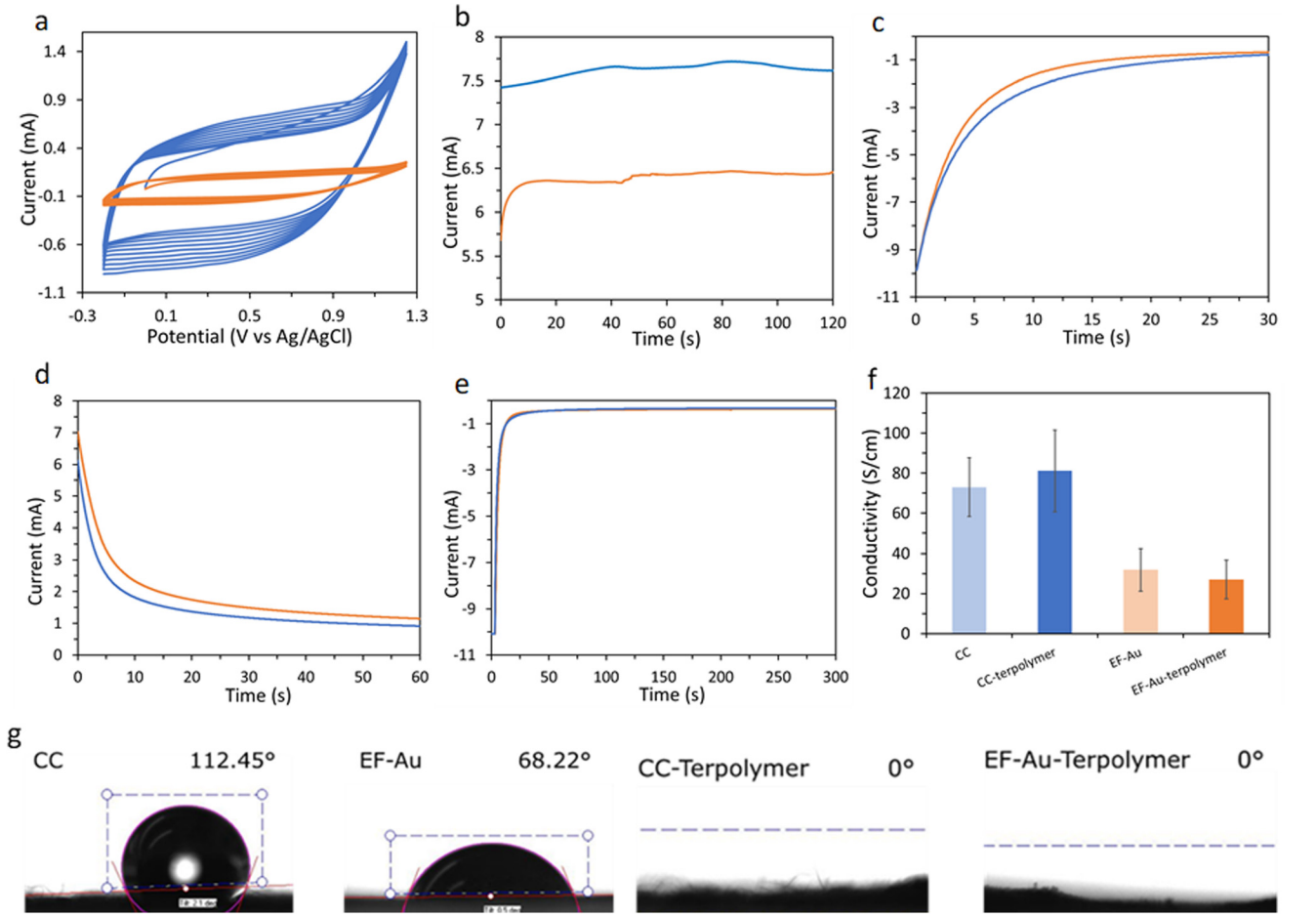

Fig. 2 (a) Potentiodynamic electropolymerization of P(EDOT-*co*-EDOTSAc-*co*-EDOTEG) on carbon cloth (CC) (blue line) and PCL elelectrospun fibers (EF) (orange line) in 0.1 M $LiClO_4$ in water : acetonitrile (1 : 1 vol : vol) at 100 mV s^{-1}, in the potential range from −0.2 to +1.25 V. (b–e) Chronoamperograms of carbon cloth (CC) (blue line) and PCL elelectrospun fibers (EF) (orange line): (b) the electropolymerization of the terpolymer P(EDOT-*co*-EDOTSAc-*co*-EDOTEG) at +1.5 V (*vs.* Ag/AgCl) for 2 min. (c) electrochemical reduction of P(EDOT-*co*-EDOTSAc-*co*-EDOTEG) at a potential of −0.8 V (*vs.* Ag/AgCl) for 30 seconds, (d) Conjugations of thiolated-ODN to the P(EDOT-*co*-EDOTSH-*co*-EDOTEG) at the potential of +1.0 V (*vs.* Ag/AgCl) for 60 s. (e) chronoamperograms of the electrochemical release of ODN at −0.8 V (*vs.* Ag/AgCl) for 5 min. (f) Electrical conductivity of the CC and the gold-coated EF mats before and after electrodeposition of P(EDOT-*co*-EDOTSAc-*co*-EDOTEG) (g) Water contact angle measurements on CC and gold-coated EF before and after electrodeposition of P(EDOT-*co*-EDOTSAc-*co*-EDOTEG).

P(EDOT-*co*-EDOTSAc-*co*-EDOTEG) (Fig. 2g). The increase in the hydrophilicity of the terpolymer-coated samples could be attributed to the presence of the hydrophilic ethylene glycol substituents on the polymer. The hydrophilic nature of the surface is expected to be advantageous in its practical biological applications, as it leads to increased wettability and decreased biofouling. The electrical conductivity of CC and gold-coated EF was measured before and after the electrodeposition of P(EDOT-*co*-EDOTSAc-*co*-EDOTEG) layer using a four-probe conductivity meter (Fig. 2f). The CC substrate showed a conductivity of 73.04 ± 14 S cm^{-1} which was higher compared to the gold-coated EF substrate (31.89 ± 10 S cm^{-1}). The conductivity of CC and EF substrates did not change significantly after the P(EDOT-*co*-EDOTSAc-*co*-EDOTEG) electrodeposition.

Scanning electron microscopy (SEM) analysis revealed the morphology of the EF and the CC before and after the electrodeposition of the terpolymer (Fig. 3). The SEM images of the bare CC (Fig. 3a–c) and EF (Fig. 3g–i) showed fibers with smooth surface morphologies.

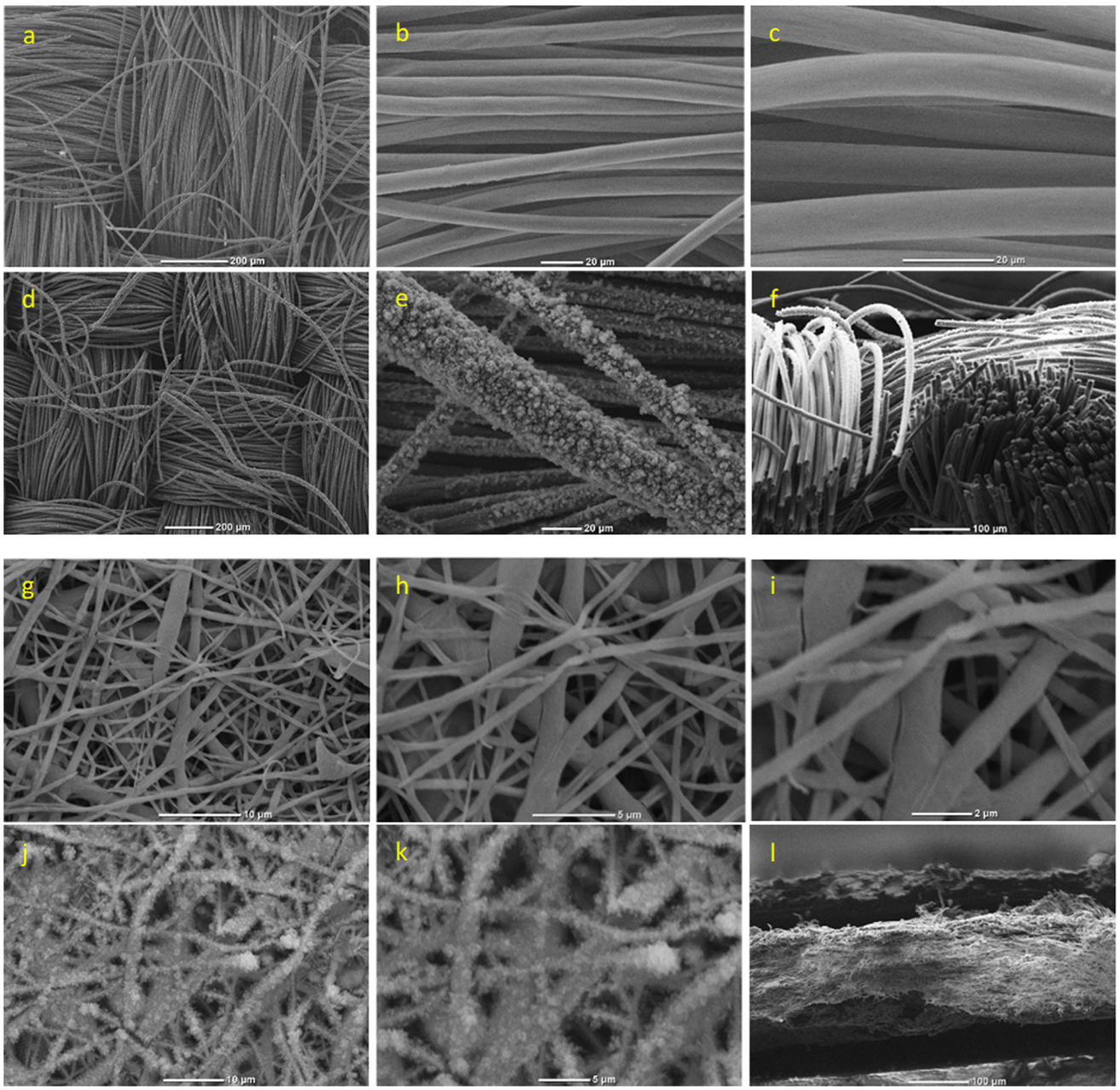

Fig. 3 SEM images of: (a–c) the uncoated carbon cloth (CC), (d and e) EDOT-*co*-EDOTSAc-*co*-EDOTEG coated CC, (f) Cross section of EDOT-*co*-EDOTSAc-*co*-EDOTEG coated CC. (g–i) uncoated electrospun fibers (EF). (j and k) EDOT-*co*-EDOTSAc-*co*-EDOTEG coated EF, (l) cross-section of EDOT-*co*-EDOTSAc-*co*-EDOTEG coated EF.

Terpolymer-coated CC (Fig. 3d–f) and EF (Fig. 3j–l) substrates showed a rougher surface morphology and uniform deposition of the conducting terpolymer. There was a significant increase in the mean diameter of CC fibers (8.71 ± 0.77 μm, n = 20) and gold-coated EF (0.84 ± 0.17 μm, n = 20) after the electrodeposition of the terpolymer to 19.9 ± 3.21 μm and 1.35 ± 0.59 μm (n = 20), respectively. This was accompanied by an increase in the surface roughness suggesting that the deposited electroactive terpolymer could contribute to a higher electrochemical activity of the substrates. In Fig. 3f, the cross-sectional SEM image of the terpolymer-coated carbon cloth displays some non-uniformity, with a thicker layer on the outermost surface, reaching depths of around 85–110 μm.

In contrast, the cross-section of terpolymer-coated electrospun fibers exhibited a prominently thick, dense, and uniform PEDOT layer on the surface of the gold-coated fibers (Fig. 3i). A minor gap, potentially stemming from electrode rupture post-treatment with liquid nitrogen, was noticeable. The PEDOT coating on the electrospun fibers had an average thickness of approximately 40–50 μm. This variation in coating thickness and distribution likely contributes to the notable difference in electrochemical response observed between the carbon cloth and the electrospun fibers. Furthermore, Fig. 2f revealed that CC was more conductive than EF. As a result, passing the same current (at constant potential) for the same amount of time deposited more terpolymer on the CC substrate. In addition, integrating the I–t curves (Fig. 2b) showed that the total charge transferred for terpolymer electropolymerization on CC (914 mC) was significantly higher than the total charge transferred for EF (760 mC), at the same constant potential of +1.5 V.

The observed increase in the CV currents (Fig. 4a) upon electrodeposition of terpolymer onto the CC and gold-coated

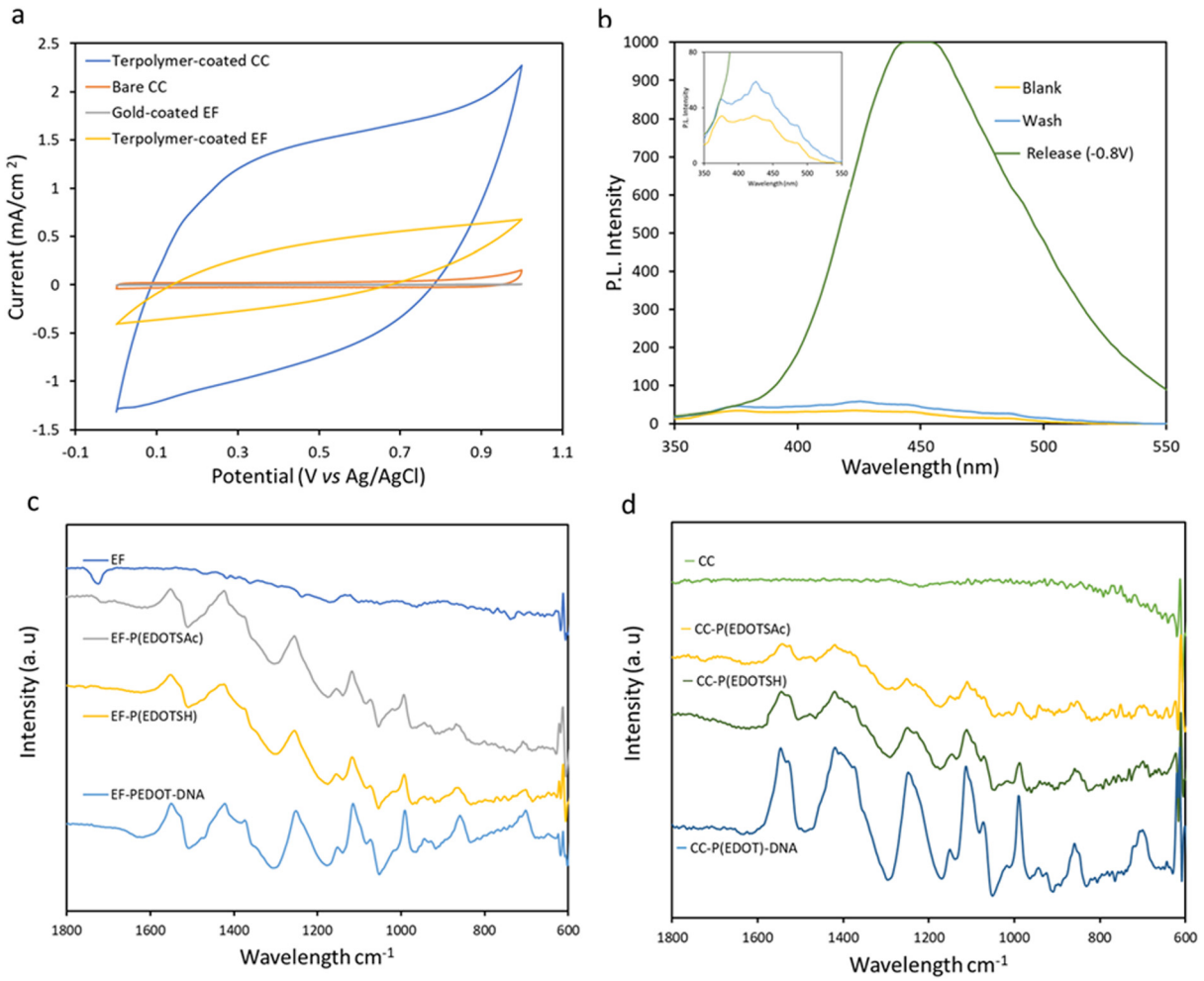

Fig. 4 (a) Cyclic voltammetry profile of the CC and gold-coated EF before and after electrodeposition of the terpolymer. (b) The fluorescence emission spectra confirming the electrochemical release of 2ME from terpolymer-coated CC (λ_{ex} = 330 nm). 2ME is conjugated by electrochemical oxidative coupling at +1.0 V (Ag/AgCl) on the CC; then, CC is kept in a PBS solution for 30 min before release (wash). 2ME was then released at −0.8 V from the CC substrate into PBS containing 1 × 10^{-3} M *o*-phthalaldehyde and alanine. PBS solution of 1 × 10^{-3} M *o*-phthalaldehyde and alanine was used as the blank sample. FTIR spectra of terpolymer coated (c) EF and (d) CC before and after electropolymerization, thiol activations and conjugation of ODN.

EF can be attributed to the deposited electroactive terpolymer. The CVs taken in PBS at a scan rate of 100 mV s^{-1} showed pseudo-rectangular CV shapes.

Based on the integrated area of the CV curves in Fig. 4a, the terpolymer-coated CC exhibited higher capacitance (7.78 ± 0.64 mF cm^{-2}) than the terpolymer-coated EF (2.11 ± 0.31 mF cm^{-2}), indicating higher electrodeposition of PEDOT on CC than on EF. At the scan rate of 100 mV s^{-1}, the capacitance of the samples completely screened the currents from redox processes. The CV profile of the terpolymer-coated samples at a lower scan rate of 5 mV s^{-1} (Fig. ESI 1†) showed a reduction peak of the terpolymer at −0.68 V.

2-Mercaptoethanol (2ME) was used as a small model molecule to demonstrate the terpolymer-coated CC-coated substrate's conjugation and release ability. A potential of +1.0 V (*vs.* Ag/AgCl) was applied to the CC in an aqueous solution of 2ME (5×10^{-3} M) containing 0.1 M $LiClO_4$ electrolyte for 1 min. Then the CC substrates were washed and kept in a 2 mL PBS solution before further use. The release of 2ME from the substrate was typically performed the next day at the constant potential of −0.8 V (*vs.* Ag/AgCl) for 5 min, followed by fluorescence detection of 2ME adduct with *o*-phthaldialdehyde and alanine in the release solution (with the maximum excitation and emission wavelengths of 330 and 450 nm, respectively).[1] The characteristic emission peak of the fluorescent adduct, with a maximum emission at 441 nm, confirmed the successful electrochemical release of 2ME from the substrate at −0.8 V (Fig. 4b). No fluorescence was observed in the absence of the electrochemical polarization, which suggests the absence of nonspecific attachment of the 2ME to the substrate.

The deposition of the terpolymer was also confirmed by FTIR of the terpolymer on EF and CC by the presence of characteristic peaks of PEDOT at 1420 cm^{-1} (C–S stretching), 1350 cm^{-1} (C–C stretching) (Fig. 4c and d) that were not present on the bare substrates.

Compared to P(EDOT) there was an additional signal for the terpolymer and P(EDOTSAc) at 1620 cm^{-1}, related to the carbonyl C═O stretching vibrations from the carbonyl present in the thioacetate of the EDOTSAc unit. After the thiol activation step, the peak at 1600 cm^{-1} disappeared, indicating the electrochemical reduction of thioacetate to –SH groups. FTIR was also carried out on the CC and EF after the conjugation of ODN. The appearance of a new peak at 1600 cm^{-1}, which could be attributed to the C═O stretching vibrations of the nucleic acid bases, confirms that the ODN has been successfully conjugated to the substrate.

Conjugation of fluorescent ODNs and their electrochemical release

The thiol groups of the terpolymer-coated CC and EF were exposed to an oxidation potential of +1.0 V for 60 s in PBS containing thiolated ODN (at a concentration of 50 μg mL^{-1}) to form disulfide linkages between the ODN and the thiolated moieties of the substrate (Fig. 1a–c). The release of the fluorescent ODN was then performed the next day by applying a potential of −0.8 V for 5 min, reducing the disulfide bonds in PBS solution back to thiol (Fig. 1c). The characteristic emission peak of the released fluorescent ODNs in PBS at 518 nm, from both functionalized CC and EF substrates, confirmed the successful conjugation and the electrochemical release of ODNs (Fig. ESI 2†).

The fluorescent intensity of the ODNs in the concentration range of 0.8 μg mL^{-1} to 0.008 μg mL^{-1} was recorded to establish the calibration graph and to quantify the amount of the released fluorescent ODNs from CC and EF substrates (Fig. 5a).

Two series of terpolymers were prepared from different termonomer feed compositions on two different substrates (CC and EF) to determine the optimum composition of the terpolymer to achieve maximum conjugation/release efficiency. Fluorescence intensity of the released ODNs from terpolymer-coated EF and CC, polymerized with different EDOTSAc : EDOTEG : EDOT ratios of 1 : 0 : 19, 1 : 2 : 17, 1 : 3 : 16, 1 : 4 : 15, 1 : 6 : 13 while keeping the concentration of EDOTSAc fixed at 5 mol%, are shown in Fig. 5b. The termonomer ratio of 1 : 3 : 16 (15 mol% EDOTEG) exhibited the highest release efficiency, which could be attributed to the presence of highly hydrophilic ethylene glycol units of EDOTEG and its antifouling properties.[8,44] With a further increase in EDOTEG concentration, the efficiency of the conjugation and release decreased for both EF and CC. Hence the 15 mol% EDOTEG was chosen as the optimized concentration of EDOTEG for the further optimization experiments.

The concentration of EDOTSAc was also optimized in another series of fluorescence ODN release experiments on EF and CC with different EDOTSAc : EDOTEG : EDOT ratios of (0 : 3 : 17, 1 : 6 : 33, 1 : 3 : 16, 2 : 3 : 16, 4 : 3 : 13) while keeping the concentration of EDOTEG fixed at 15 mol% (Fig. 5c). The fluorescence intensity of released ODN increased up to termonomer ratio of 1 : 3 : 16 (5 mol% of EDOTSAc), but decreased at higher EDOTSAc ratios. This could be attributed to the reduction of spacing between EDOTSAc units, leading to steric blocking caused by the high density of ODN on the surface, or self-reactivity of the SH groups at densities beyond 5%.

Accordingly, the optimal spacing between EDOTSAc units on the surface is a crucial parameter to achieve a highly efficient conjugation and release from CC and EF. A termonomer ratio of 1 : 3 : 16 containing 2.52 mM EDOTSAc (5%) : 5.05 mM EDOTEG (15%) : 44.7 mM EDOT (80%) was chosen as the optimal composition for subsequent experiments.

Release potential and release time are the key parameters affecting release efficiency. Fluorescent ODNs were released at −0.8 V in PBS in 4 × 5 min cycles. As shown in Fig. 5d, the first release cycle resulted in a strong fluorescence signal, while further second and third 5 min polarization of the substrate at −0.8 V resulted in lower fluorescence signals. A low fluorescence signal was recorded for the EF and CC substrates when no potential was applied to both substrates, indicating very low nonspecific adsorption of the ODN to the substrates, confirming the success of the electrochemically controlled

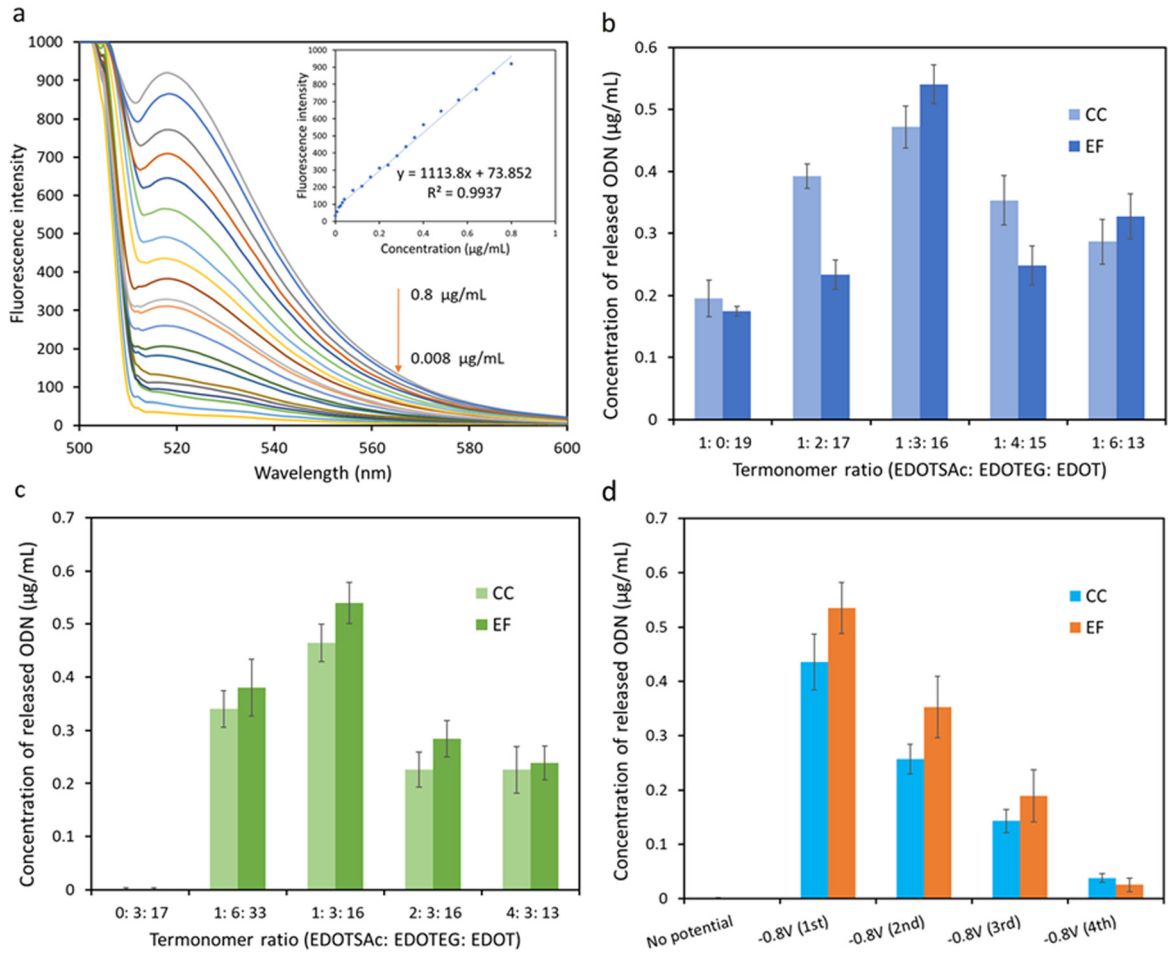

Fig. 5 (a) The fluorescent intensity of fluorescently labelled connexin43 ODN in the concentration range from 0.8 μg mL^{-1} to 0.008 μg mL^{-1} and calibration curve of connexin43 ODN concentrations in PBS *vs*. fluorescence intensity. (b) The concentration of fluorescent connexin43 DNA oligo (ODN) released from the terpolymer-functionalized EF and CC upon optimization of the ratio of EDOTEG in the termonomer feed, while the ratio of EDOTSAc was constant at 5 mol%. (c) The concentration of fluorescent connexin43 of ODN released from the terpolymer-functionalized EF and CC upon optimization of the ratio of EDOTSAc in the termonomer feed, while the ratio of EDOTEG was constant at 15 mol%. (d) The concentrations of released connexin43 ODNs from terpolymer-coated EF and CC with the optimized terpolymer composition (λ_{ex} = 493 nm). The release of fluorescent ODN was performed at −0.8 V in PBS in 4 × 5 min cycles (n = 3).

conjugation/release (Fig. 5d). The results also indicated that the EF showed slightly higher release during the first and second release cycles than CC (Fig. ESI 3†). The estimated density of connexin43 units per unit surface area with the optimized terpolymer composition was approximately 1.98 ± 0.17 pmol mm^{-2} for carbon cloth (CC) and 2.48 ± 0.29 pmol mm^{-2} for electrospun fibers (EF).

The termonomer EDOTSAc : EDOTEG : EDOT ratio of 1 : 3 : 16 was also utilised for the conjugation and release of non-fluorescent ODN, measured using the NanoDrop (Fig. ESI 3c†). The measurements taken using the spectrofluorometer and NanoDrop showed a discrepancy in the maximum concentration of ODN released from the EF and CC substrates (Fig. 5d *vs.* Fig. ESI 3c†). There is a discrepancy between the measured concentrations with spectrofluorometer (maximum of 0.54 ± 0.04 μg mL^{-1} for the EF substrate and 0.43 ± 0.05 μg mL^{-1} for the CC substrate) and NanoDrop (maximum concentration of 2.26 ± 0.19 μg mL^{-1} for the EF and 1.52 ± 0.24 μg mL^{-1} for the CC substrates) (Fig. ESI 3c†). It has been reported previously that NanoDrop method, which measures absorbed light at 260 nm, tends to overestimate ODN concentrations, hence we believe fluorescence spectrophotometry provided more sensitive and specific measurements of the ODN concentration.[50–52]

Conclusion

We have developed an electrochemical system based on a highly porous and flexible carbon cloth and electrospun substrates functionalized with a conducting terpolymer P(EDOT-*co*-EDOTSAc-*co*-EDOTEG) for the covalent conjugation and release of connexin43 antisense as an model drug and a reported wound healing agent. The conjugation was facilitated

by the electrochemical oxidative coupling of the thiols present on the substrates and on the drug molecule, while reduction of the formed disulfide bond afforded electrochemical controlled of the drug release. The disulfide bond between both of the investigated substrates (EF AND CC) substrate and the conjugated connexin43 antisense cleaved at a mild potential of −0.8 V (*vs.* Ag/AgCl) applied for a short time (300 s). This novel, flexible, porous and general platform technology holds a great potential in wound dressing and other drug-delivery applications.

Author contributions

The manuscript was written through the contributions of all authors. All authors have given approval for the final version of the manuscript.

Conflicts of interest

There are no conflicts to declare.

Acknowledgements

The authors would like to acknowledge the financial support from the Faculty of Science Fostering Collaborations Fund.

References

1 A. Akbarinejad, C. L. Hisey, M. Martinez-Calderón, J. Low, D. T. Bryant, B. Zhu, D. Brewster, E. W. C. Chan, J. Ashraf and Z. Wan, *Adv. Mater. Interfaces*, 2022, **9**, 2102475.
2 E. Krieg, K. Gupta, A. Dahl, M. Lesche, S. Boye, A. Lederer and W. M. Shih, *Commun. Biol.*, 2020, **3**, 1–9.
3 J. K. Patra, G. Das, L. F. Fraceto, E. V. R. Campos, M. D. P. Rodriguez-Torres, L. S. Acosta-Torres, L. A. Diaz-Torres, R. Grillo, M. K. Swamy and S. Sharma, *J. Nanobiotechnol.*, 2018, **16**, 1–33.
4 R. Prodromou, K. N. Day, S. Saberi-Bosari, J. D. Schneible, M. D. Mabe, A. San Miguel, M. A. Daniele, V. Pozdin and S. Menegatti, *Adv. Funct. Mater.*, 2021, **31**, 2101410.
5 J. Moratz, A. Samanta, J. Voskuhl, S. K. Mohan Nalluri and B. J. Ravoo, *Chem. – Eur. J.*, 2015, **21**, 3271–3277.
6 R. Weinstain, T. Slanina, D. Kand and P. Klan, *Chem. Rev.*, 2020, **120**, 13135–13272.
7 L. R. Staben, S. G. Koenig, S. M. Lehar, R. Vandlen, D. Zhang, J. Chuh, S.-F. Yu, C. Ng, J. Guo and Y. Liu, *Nat. Chem.*, 2016, **8**, 1112–1119.
8 J. Ashraf, A. Akbarinejad, C. L. Hisey, D. T. Bryant, J. Wang, B. Zhu, C. W. Evans, D. E. Williams, L. W. Chamley and D. Barker, *ACS Appl. Mater. Interfaces*, 2022, **14**, 32880–32889.
9 A. Akbarinejad, C. L. Hisey, D. Brewster, J. Ashraf, V. Chang, S. Sabet, Y. Nursalim, V. Lucarelli, C. Blenkiron and L. Chamley, *ACS Appl. Mater. Interfaces*, 2020, **12**, 39005–39013.
10 Y. Song, Y. Shi, M. Huang, W. Wang, Y. Wang, J. Cheng, Z. Lei, Z. Zhu and C. Yang, *Angew. Chem., Int. Ed.*, 2019, **58**, 2236–2240.
11 H. Shen, R. Su, J. Peng, L. Zhu, K. Deng, Q. Niu, Y. Song, L. Yang, L. Wu and Z. Zhu, *Bioact. Mater.*, 2022, **11**, 32–40.
12 T. Gao, T. Chen, C. Feng, X. He, C. Mu, J.-I. Anzai and G. Li, *Nat. Commun.*, 2019, **10**, 1–10.
13 R. J. Pj, O. S. Oluwafemi, S. Thomas and A. Oyedeji, *J. Drug Delivery Sci. Technol.*, 2022, 103390.
14 L. Xu, Y. Yang, Y. Mao and Z. Li, *Adv. Mater. Technol.*, 2022, **7**, 2100055.
15 K. Tybrandt, K. C. Larsson, S. Kurup, D. T. Simon, P. Kjäll, J. Isaksson, M. Sandberg, E. W. Jager, A. Richter-Dahlfors and M. Berggren, *Adv. Mater.*, 2009, **21**, 4442–4446.
16 N.-N. Lu, M. Xie, J. Wang, S.-W. Lv, J.-S. Yi, W.-G. Dong and W.-H. Huang, *ACS Appl. Mater. Interfaces*, 2015, **7**, 8817–8826.
17 D. Ou, D. Sun, Z. Liang, B. Chen, X. Lin and Z. Chen, *Sens. Actuators, B*, 2019, **285**, 398–404.
18 S. Mura, J. Nicolas and P. Couvreur, *Nat. Mater.*, 2013, **12**, 991–1003.
19 C. M. Wells, M. Harris, L. Choi, V. P. Murali, F. D. Guerra and J. A. Jennings, *J. Funct. Biomater.*, 2019, **10**, 34.
20 L. Feng, L. Xu, S. Dong and J. Hao, *Soft Matter*, 2016, **12**, 7495–7504.
21 S. K. M. Nalluri, J. Voskuhl, J. B. Bultema, E. J. Boekema and B. J. Ravoo, *Angew. Chem., Int. Ed.*, 2011, **50**, 9747–9751.
22 C. Gong, X. Mao, Z. Wang, Z. Luo, Z. Liu, Y. Ben, W. Zhang and Z. Guo, *Front. Bioeng. Biotechnol.*, 2022, **10**, 891727.
23 T. Nakagawa, R. Hashimoto, K. Maruyama, T. Tanaka, H. Takeyama and T. Matsunaga, *Biotechnol. Bioeng.*, 2006, **94**, 862–868.
24 H. Sun, X. Zhu, L. Zhang, Y. Zhang and D. Wang, *Mater. Sci. Eng., C*, 2010, **30**, 311–315.
25 J. Moratz, L. Stricker, S. Engel and B. J. Ravoo, *Macromol. Rapid Commun.*, 2018, **39**, 1700256.
26 L. Xu, L. Feng, J. Hao and S. Dong, *ACS Appl. Mater. Interfaces*, 2015, **7**, 8876–8885.
27 W. Y. Hong, S. H. Jeon, E. S. Lee and Y. Cho, *Biomaterials*, 2014, **35**, 9573–9580.
28 B. Zhu, D. T. Bryant, A. Akbarinejad, J. Travas-Sejdic and L. I. Pilkington, *Polym. Chem.*, 2022, **13**, 508–516.
29 M. R. Abidian, D. H. Kim and D. C. Martin, *Adv. Mater.*, 2006, **18**, 405–409.
30 T. Gao, L. Li, B. Wang, J. Zhi, Y. Xiang and G. Li, *Anal. Chem.*, 2016, **88**, 9996–10001.
31 Z. Yuan, J. Wang, Y. Wang, Y. Zhong, X. Zhang, L. Li, J. Wang, S. F. Lincoln and X. Guo, *Macromolecules*, 2019, **52**, 1400–1407.
32 C. Jiao, F. Obst, M. Geisler, Y. Che, A. Richter, D. Appelhans, J. Gaitzsch and B. Voit, *Polymers*, 2022, **14**, 267.
33 J. J. Kim, Y. Wang, H. Wang, S. Lee, T. Yokota and T. Someya, *Adv. Funct. Mater.*, 2021, **31**, 2009602.
34 Y. Liu, M. Pharr and G. A. Salvatore, *ACS Nano*, 2017, **11**, 9614–9635.

35 F. Chen, Q. Huang and Z. Zheng, *Small Struct.*, 2022, **3**, 2100135.
36 C. K. Sen, G. M. Gordillo, S. Roy, R. Kirsner, L. Lambert, T. K. Hunt, F. Gottrup, G. C. Gurtner and M. T. Longaker, *Wound Repair Regen.*, 2009, **17**, 763–771.
37 G. C. Gurtner, S. Werner, Y. Barrandon and M. T. Longaker, *Nature*, 2008, **453**, 314–321.
38 A. T. Barker, L. F. Jaffe and J. J. W. Vanable, *American Journal of Physiology-Regulatory, Integrative and Comparative Physiology*, 1982, **242**, R358–R366.
39 R. T. Beyene, S. L. Derryberry and A. Barbul, *Surg. Clin.*, 2020, **100**, 695–705.
40 J. Anjana, V. K. Rajan, R. Biswas and R. Jayakumar, *Curr. Pharm. Des.*, 2017, **23**, 3529–3537.
41 H. Rodríguez-Acosta, J. M. Tapia-Rivera, A. Guerrero-Guzmán, E. Hernández-Elizarraráz, J. A. Hernández-Díaz, J. J. Garza-García, P. E. Pérez-Ramírez, S. F. Velasco-Ramírez, A. C. Ramírez-Anguiano and G. Velázquez-Juárez, *J. Tissue Viability*, 2022, **31**, 173–179.
42 H. S. Yang, J. Shin, S. H. Bhang, J.-Y. Shin, J. Park, G.-I. Im, C.-S. Kim and B.-S. Kim, *Exp. Mol. Med.*, 2011, **43**, 622–629.
43 J. Tian, H. Feng, L. Yan, M. Yu, H. Ouyang, H. Li, W. Jiang, Y. Jin, G. Zhu and Z. Li, *Nano Energy*, 2017, **36**, 241–249.
44 J. Ashraf, S. Lau, A. Akbarinejad, D. T. Bryant, L. W. Chamley, L. I. Pilkington, D. Barker, D. E. Williams, C. W. Evans and J. Travas-Sejdic, *ACS Appl. Nano Mater.*, 2023, 3981–3989.
45 J. Ashraf, S. Lau, A. Akbarinejad, D. T. Bryant, L. W. Chamley, L. I. Pilkington, D. Barker, D. E. Williams, C. W. Evans and J. Travas-Sejdic, *ACS Appl. Nano Mater.*, 2023, **6**, 3981–3989.
46 L. Y. Law, W. V. Zhang, N. S. Stott, D. L. Becker and C. R. Green, *J. Biomol. Tech.*, 2006, **17**, 270.
47 R. Mori, K. T. Power, C. M. Wang, P. Martin and D. L. Becker, *J. Cell Sci.*, 2006, **119**, 5193–5203.
48 C. Qiu, P. Coutinho, S. Frank, S. Franke, L.-Y. Law, P. Martin, C. R. Green and D. L. Becker, *Curr. Biol.*, 2003, **13**, 1697–1703.
49 M. Khandaker, H. Nomhwange, H. Progri, S. Nikfarjam and M. B. Vaughan, *Bioengineering*, 2022, **9**, 19.
50 B. Bruijns, T. Hoekema, L. Oomens, R. Tiggelaar and H. Gardeniers, *Analytica*, 2022, **3**, 371–384.
51 M. Simbolo, M. Gottardi, V. Corbo, M. Fassan, A. Mafficini, G. Malpeli, R. T. Lawlor and A. Scarpa, *PLoS One*, 2013, **8**, e62692.
52 M. O'neill, J. McPartlin, K. Arthure, S. Riedel and N. McMillan, *J. Phys.*, 2011, **307**, 012047.